Sixth International Symposium on Marine Propulsors
smp'19, Rome, Italy, May 2019

Mechanisms of Low-Frequency Broadband Noise by Cavitating Tip-Vortices on Marine Propellers

Johan Bosschers

Maritime Research Institute Netherlands (MARIN), Wageningen, The Netherlands

ABSTRACT

Comfort on board has become an important aspect in the design of ships over the last decades, especially comfort for passengers on cruise vessels and for owners of yachts. Therefore, cavitation on propellers for these ships should be minimized, leaving often only a tip-vortex cavity. However, tip-vortex cavitation is known to be a cause of broadband pressure fluctuations on the hull above the propeller, typically in a frequency range between 30 and 100 Hz. The present paper discusses the mechanisms involved in generating these low-frequency broadband hull fluctuations which also describe the underwater radiated noise.

Keywords

Propeller, cavitation, tip vortex, hull pressures, underwater radiated noise

1 INTRODUCTION

Noise and vibration onboard ships are important for comfort of crew and passengers. Especially passengers on cruise vessels and owners of yachts require high comfort levels. An important source of noise and vibration is cavitation on the ship propeller. The collapse of cavitation generates pressure fluctuations that excite the ship hull above the propeller. Noise reduction is usually achieved by unloading the propeller tip and decreasing sheet cavitation as much as possible. This leaves often only tip vortex cavitation on the propeller. However, this type of cavitation generates broadband hull pressure fluctuations (HPF) which may lead to ship vibration issues (Brubakk & Smogeli 1988, Carlton 2015). The broadband hull pressure fluctuations are typically seen as a hump in the spectrum in a frequency range between 30 Hz and 100 Hz. The same hump can also be observed in the underwater radiated noise (URN).

Broadband spectra of HPF as measured on model scale for twin-screw vessels were presented by Friesch (1998), Frechou *et al.* (2000), Kuiper (2001), van Terwisga *et al.* (2007), and Bosschers (2009a), and the topic is briefly addressed by the 23rd ITTC Specialist Committee on Cavitation Induced Pressures (2002). Consensus is that broadband HPF is related to the cavitating tip vortex and that variability of the cavitation collapse between blade passages is of importance, though the physical mechanisms are still not fully understood. Bosschers (2009a) relates the centre frequency of the hump to a resonance frequency obtained from the dispersion relation of deformations of the cavity interface. Pennings *et al.* (2016) show that the frequency of the oscillations of the volume of a propeller tip-vortex cavity, determined by high-speed video, is identical to the most dominant frequency in the noise spectrum.

Semi-empirical model for the (broadband) noise of tip-vortex cavitation have been developed by, among others, Raestad (1996) and Bosschers (2018a). These models relate the broadband noise to the thickness of the tip-vortex cavity computed by a potential flow method and a simple vortex model. Raestad (1996) predicts the inboard noise while Bosschers (2018a) predicts the broadband HPF and URN.

The relation between broadband noise and tip-vortex cavitation is illustrated by the CFD results of Fujiyama and Nakashima (2017). They compute the HPF for the single-screw vessel Seiun-Maru for two different propeller geometries. Computational results, obtained at a model-test Reynolds number and corrected by a scaling rule for URN, showed good agreement with full-scale measurement data with respect to the broadband part. However, computations at the full-scale Reynolds number, in which sheet cavitation was predicted but the tip-vortex cavity was not captured, showed a significant underprediction of the levels of the broadband noise, especially for the propeller of conventional planform. These results show that, for this ship, the broadband hump of the spectrum, centred around 50 Hz, is mainly due to tip-vortex cavitation.

Very large broadband noise levels are known to occur when a controllable-pitch propeller is operating at reduced pitch setting in order to achieve low ship speed. These broadband noise levels are due to the interaction of two counter-rotating vortices. Okamura *et al.* (1994) present the broadband noise spectrum as measured in a cavitation tunnel, Berghult (2000) has developed an empirical formulation for the broadband noise levels as function of pitch offset and blade area ratio, and Carlton

(2015) shows the interacting cavitating vortices and resulting vibration level at full-scale.

The topic of propeller tip-vortex cavitation and its broadband noise is discussed in detail in the thesis by Bosschers (2018b). The present paper provides a short review of the main mechanisms involved and is extracted from that thesis. First, some fundamental research on a vortex cavity and on broadband noise are discussed: Chapter 2 very briefly presents some aspects of the dynamics of vortex cavitation, focusing on the presence of a resonance frequency; Chapter 3 discusses the vortex cavity as a noise source and shows how variability between blade passages generates the broadband part of the spectrum. Some applied research is presented thereafter: The structure of vortex cavitation is discussed in Chapter 4 focusing on an attached tip-vortex cavitation and on a sheet cavity in the tip area of a skewed propeller blade. The excitation mechanism of an attached tip-vortex cavity that leads to a broadband spectrum is presented in Chapter 5, and the concluding remarks are given in Chapter 6.

2 DYNAMICS OF VORTEX CAVITATION

2.1 Dynamics in 2-D viscous flow

The dynamics of a vortex cavity in 2-D inviscid flow was investigated by Ligneul *et al.* (1983) whereas the dynamics in 2-D viscous flow was studied by Chahine (1995). In Bosschers (2009b), the cavity dynamics was also studied in 2-D viscous flow, but with the boundary condition at the cavity interface corresponding to a zero shear stress condition. This boundary condition, first derived by Bosschers *et al.* (2008), shows acceptable agreement with PIV measurements on a cavitating tip vortex by Pennings *et al.* (2015) as shown in detail by Bosschers (2018c). An example of a result is presented in Figure 1. Both experimental and theoretical results show that further away from the cavity the azimuthal velocity distribution for non-cavitating and cavitating flow is identical. However, at the cavity interface a vorticity region is present that leads to a difference in azimuthal velocity between non-cavitating and cavitating flow. If, in the theoretical model, the growth of the viscous core size for cavitating flow is identical to that for non-cavitating flow (results in Figure 1 for f=1.0), the thickness of this vorticity region is too small. If the growth is larger (by a factor f= 1.6), the results of the theoretical model agree well with the experimental data.

A typical example of the time trace of the cavity radius from an unsteady computation is presented in Figure 2a. The solution was initialized with the analytical model for a 2-D vortex cavity (Bosschers 2009b, Bosschers 2018c), and at the first time step the pressure is slightly increased after which it remains constant. This issufficient for the vortex cavity to come into resonance.

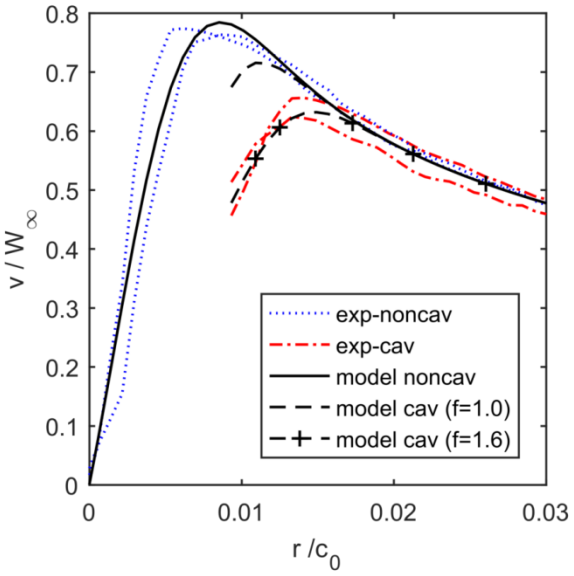

Figure 1. Comparison of the azimuthal velocity distribution with radial distance to vortex centre between experimental data of Pennings (2015b) and the analytical model for a cavitating vortex, Bosschers (2018c).

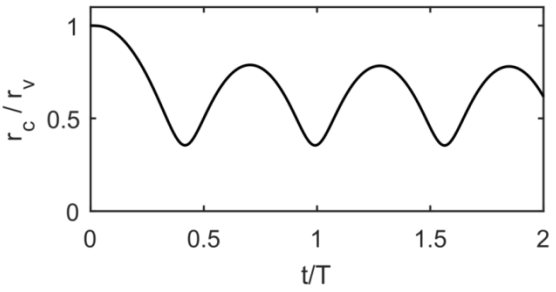

a. Time trace of cavity size r_c, made non-dimensional with the viscous core size for non-cavitating flow r_v

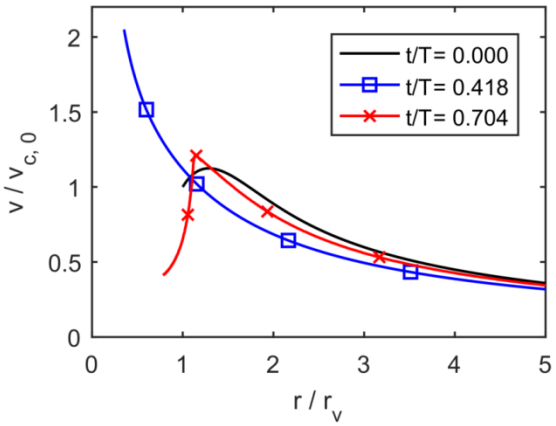

b. Azimuthal velocity distribution at three time steps

Figure 2. Results of computations of a vortex cavity in 2-D unsteady incompressible viscous flow.

The azimuthal velocity distribution at three time steps is provided in Figure 2b. The collapse of the cavity is fully inertia driven as a large increase in azimuthal velocity near the cavity interface is observed. Viscous effects at minimum cavity radius (t/T= 0.418) are limited to a very small region near the cavity interface that cannot be identified from this graph. At the rebound (t/T= 0.704), the viscous effects are again visible in the region just outside the cavity.

Assuming small perturbations of the cavity size, a formulation for the resonance frequency of a vortex cavity can be derived for 2-D viscous flow, analogous to the derivation for inviscid flow presented by Franc and Michel (2004). The formulation for the resonance frequency f of a vortex cavity with mean cavity radius $\bar{r}_c$ reads

$$\left(\frac{2\pi f \bar{r}_c}{W}\right)^2 = K_\sigma \frac{1}{\ln\left(r_{ref}/\bar{r}_c\right)}, \qquad (1)$$

with W the reference velocity and r_{ref} the reference radius where the pressure is prescribed, see Bosschers (2018b) for more details. Parameter K_σ is the 'stiffness-coefficient', for which two formulations were derived using the azimuthal velocity distribution of a non-cavitating vortex as given Rosenhead (1931),

$$K_{\sigma,1} = \frac{\sigma_W}{1+\left(\bar{r}_c/r_v\right)^2}, \qquad (2)$$

$$K_{\sigma,2} = \left(\frac{v_c}{W}\right)^2. \qquad (3)$$

The first formulation uses the cavitation number $\sigma_W = \left(p_\infty - p_v\right)/\frac{1}{2}\rho W^2$ and the viscous core size in non-cavitating flow r_v. The second formulation uses the azimuthal velocity component at the cavity interface, v_c. It is shown in Bosschers (2018b) that these formulations give a reasonable prediction of the resonance frequency as obtained from 2-D computations.

2.2 Dynamics in 3-D flow

In 3-D flow, the situation is more complicated. Analysis of perturbations of the cavity interface for 3-D inviscid flow leads to an analytical formulation for a dispersion relation that provides the relation between frequency and spatial wave number of the perturbation. This relation, first derived by Lord Kelvin (Thomsom 1880), shows that all perturbations are neutrally stable and that, therefore, a criterion for a resonance frequency cannot directly be derived. Experimental evidence of this dispersion relation has been presented by Pennings *et al.* (2015).

Several hypotheses for criteria for resonance, making use of the derived dispersion relation, are discussed by Bosschers (2018b). When plotting these criteria for the resonance frequency as function of cavitation number, the relation between frequency, cavity size and cavitation number for these criteria is somewhat similar to Eq. (1) and (2). One of these hypotheses is the zero-group speed condition for the mode that considers the axisymmetric cavity volume variation. This criterion is compared in Figure 3 with experimental data for the resonance frequency of the 'singing vortex' of Maines and Arndt (1997). The 'singing vortex' is a cavitating tip-vortex trailing from the tip of wing with elliptical planform. In specific conditions, this vortex cavity generates a tonal noise of which the exact mechanisms involved are still unknown (Arndt *et al.* 2015). The results for the theoretical formulation shown in Figure 3 have been derived for potential flow theory, and for potential flow theory with ad-hoc viscous correction. The theoretical values for the resonance frequency are in good agreement with the measured values which provides some confidence in the applied criterion but further investigation is required.

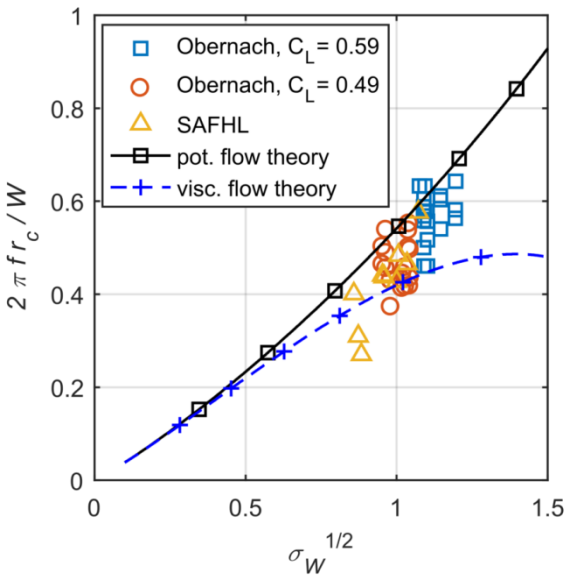

Figure 3. Comparison between the measured frequency of the singing vortex (Maines and Arndt 1997) and the criterion for zero group speed obtained from the dispersion relation of a vortex cavity.

3 VORTEX CAVITY AS A NOISE SOURCE

3.1 A cylindrical noise source of finite extent

We now consider the vortex cavity as an infinite cylinder of radius r_c that vibrates over a length $2L$ with amplitude $\hat{r}$ and angular frequency ω. The deformation of the cylinder is axisymmetric and varies in axial direction as $r' = \hat{r}\cos\left(k_0 z\right) = \hat{r}\cos\left(\pi z/2L\right)$ for $|z| < L$. The z-coordinate is along the axis of the cylinder and k_0 is the flexural wave number of the cylinder deformation along the z-axis with wave length equal to $4L$. The formulation for the radiated noise by such a cylindrical noise source can be derived using the approach given by Junger and Feith (1986). Use is made of the method of stationary phase assuming that the pressure is analyzed in the far field and that the source is acoustically compact. The

radiated pressure at distance R and polar angle ϑ from the centre of the cylinder is then given by

$$\hat{p}(R,\vartheta) = \rho\omega^2 \frac{r_c \hat{r}}{\pi} \frac{\exp(ikR)}{R} \left[\frac{(k_0 L)^2 \cos(kL\cos\vartheta)}{(k_0 L)^2 - (kL\cos\vartheta)^2} \right] \qquad (4)$$

with k the acoustic wave number, $k = \omega/c$.

The directivity of Eq.(4) is presented in Figure 4 for three frequencies. At low frequencies, where the broadband noise due to the collapse of the large-scale vortex-cavity is generated, the vortex cavity can be considered as a monopole as the directivity is very small: For $L = 0.25\text{m}$, the frequency corresponding to $kL = \pi/2$ corresponds to $f = 1500\,\text{Hz}$. At higher frequencies the radiated noise is no longer omni-directional, but at these frequencies the smaller bubbles generated by the collapse of the vortex-cavity are also expected to contribute to the radiated noise. For reference purposes, Figure 4 also shows the directivity of a dipole.

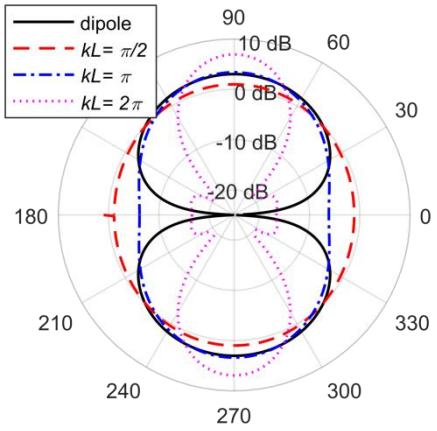

Figure 4. Directivity plot for angle ϑ for $k_0 L = \pi/2$. The vortex axis runs along $\vartheta = 0\,\text{deg}$ and $\vartheta = 180\,\text{deg}$.

3.2 Influence of variability between blade passages

We consider here the broadband noise at low frequencies generated by the collapse of cavitation on marine propellers. The maximum extent of cavitation, followed by the collapse, is related to the passage of the propeller blade through the location of minimum axial velocity in the ship wake field. Multiple blade passages lead to a periodic signal. If the signal is perfectly periodical, the Fourier transform would only show components at the blade passage frequency and harmonics thereof. In reality, the cavity collapse is not exactly periodical but varies between blade passages and this leads to a broadband signal as discussed by e.g. Baiter *et al.* (1982) and Bark (2000). From a mathematical point of view, this is well shown by the formulations derived by MacFarlane (1949) for variability of amplitude and of time shift of the signal between blade passages. The effect of combined

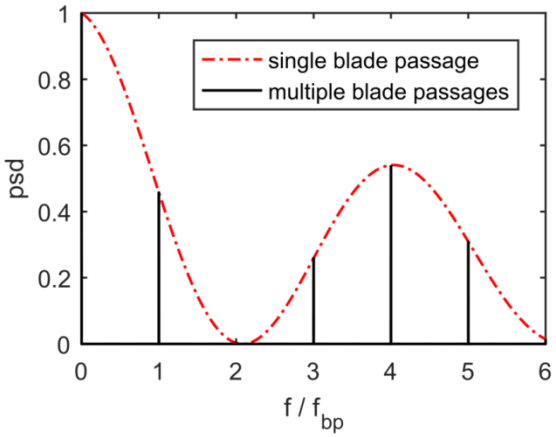

a. Perfect repetitive blade passages

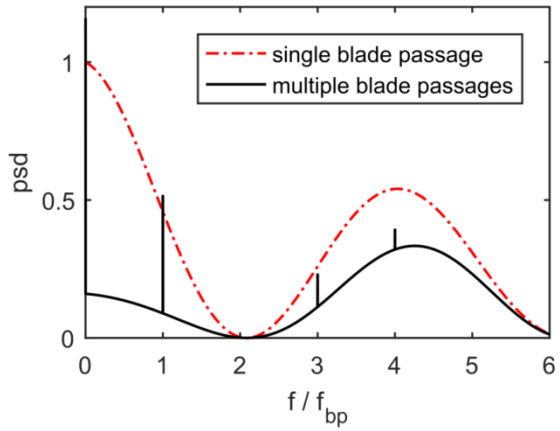

b. Variation in amplitude and phase between blade passages

Figure 5. Effect of amplitude and phase angle variation of the cavity collapse of multiple blade passages on the spectrum

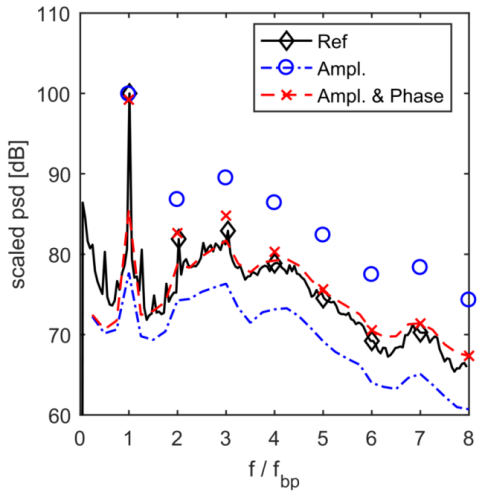

Figure 6. Example of a (normalized) hull-pressure spectrum of a twin-screw vessel.

variability of amplitude and time shift, which can also be interpreted as variability of phase, is derived by Bosschers (2018b).

The variation in amplitude and time are assumed independent and are described by Gaussian probability distributions with standard deviation σ_a and σ_τ for amplitude and time, respectively. The mean spectrum is given by $\bar{a}_n^2 |G(\omega)|^2$ with ω the angular frequency. The power spectral density is then given by

$$R(\omega) = \left\{ \sigma_a^2 + \bar{a}_n^2 \left[1 - \exp\left(-\omega^2 \sigma_\tau^2\right) \right] + \bar{a}_n^2 \exp\left(-\omega^2 \sigma_\tau^2\right) \Delta(\omega/\omega_r) \right\} |G(\omega)|^2 \quad (5)$$

where $\Delta(\omega/\omega_r)$ denotes the Dirac-comb and ω_r corresponds to the angular blade rate frequency.

A stylized spectrum showing the effect of amplitude and time or phase is shown in Figure 5 where f_{bp} denotes the circular blade passage frequency. The red line is the stylized spectrum of a single blade passage. The black line is the spectrum of a perfect repetitive signal in Figure 5a, or a signal with varying amplitude and phase as shown in Figure 5b. The latter clearly shows the broadband hump. Simultaneously with the increase in broadband energy, the amplitudes at the tonals decrease with increasing frequency. The broadband hump in the spectrum of the single blade passage is considered to be due to the finite extent of the dampened oscillatory behavior of the cavity collapse and rebounds.

Equation (5) has also be used to analyze a measured hull pressure spectrum due to a cavitating propeller during sea trials. The reference spectrum, computed for the whole time trace using overlapping time series and a Hanning window is presented in Figure 6 where it is denoted by 'Ref'. Using the average shaft revolution period, the spectrum of each shaft revolution has been computed which gives the distribution of amplitude and phase with frequency. From these spectra, the average power density spectrum and the standard deviation of amplitude and phase can be computed. The resulting power density spectrum is denoted by 'Ampl' in Figure 6. The spectrum consists of tonals at harmonics of the blade passage frequency, computed from the average amplitudes, and a broadband part computed from the standard deviation of the amplitude. Correcting this spectrum for the effect of variability in phase angle results in the spectrum denoted by 'Ampl. & Phase'. This spectrum is identical to the reference spectrum showing that Eq. (5) is a correct representation of the effect of variability of amplitude and phase and that this variability is indeed the source of the broadband hump.

4 CAVITATION PATTERNS

4.1 Detached / attached tip-vortex cavity

A detached tip-vortex cavity refers to the situation that the inception of tip-vortex cavitation occurs downstream of the tip of the hydrofoil or of the propeller. This tip-vortex cavity has a cylindrical shape and is shown in Figure 7, Case 1. When the inception of cavitation occurs on the blade, one speaks of an attached tip-vortex cavity. It first forms a small, probably closed, sheet cavity on the blade, possibly in combination with an elliptical cross-section of the vortex cavity. Such a cavity pattern is shown in Figure 7, Case 2, and is schematically illustrated in Figure 8.

The non-dimensional hull-pressure spectra for both cases for a transducer directly above the propeller centre are presented in Figure 7, lower graph. The attached vortex cavity generates significant higher broadband noise than the detached vortex cavity.

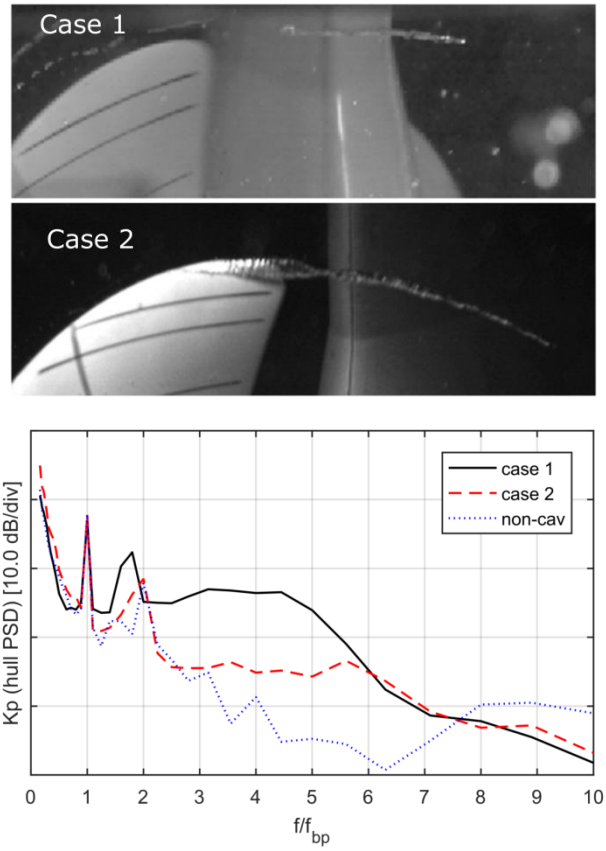

Figure 7. Example of an detached tip-vortex cavity (Case 1) and an attached tip-vortex cavity (Case 2) and the resulting non-dimensional hull-pressure spectrum. The observations and measurements are for a podded propeller and have been made in the Depressurized Wave Basin of MARIN.

The closed cavity on the blade that turns into the vortex cavity shows a resemblance with the *Chaplygin-Lamb vortex dipole* (Meleshko & van Heijst, 1994), which describes a 2-D circular vortex consisting of two regions with opposite vorticity while the vorticity equals zero outside these regions. Such a vortex also describes a semi-cylindrical inviscid vortex on a flat rigid wall. For the vortex cavity, we can assume that vorticity is present within the cavity and, therefore, that this vorticity is also present in the cavity that is attached to the blade. Because of the solid-wall boundary condition, this vorticity is mirrored in the blade surface leading to a cavity interface that has a semi-cylindrical shape that at the trailing edge of the blade turns into an elliptical vortex cavity. Such an elliptical cross-section can also clearly be observed in the

dispersion diagram of a tip-vortex cavity, see Bosschers (2018b).

4.2 Closure-vortex cavity from sheet cavitation

At higher tip loading, sheet cavitation will be present at the tip of the hydrofoil or of the propeller. The sheet-cavity is usually closed by a re-entrant jet or, if the jet becomes more oriented in spanwise direction, a side-entrant jet (Foeth *et al.*, 2008). The re-entrant jet and side-entrant jet lead to an open structure of the cavity at its closure region, as schematically shown in Figure 9. Within the re-entrant jet and side-entrant jet, the liquid evaporates. In the sheet cavity, a so-called *cavity-closure vortex* is formed as described by Bark and Bensow (2013) in their description of cavity structures in relation to cavitation erosion. When the sheet cavity collapses, this cavity-closure vortex may form a *closure-vortex cavity*, as defined here. Because this vortex cavity is formed by the sheet and not by the vortex circulation, the cavity is not in equilibrium and will therefore collapse. It is hypothesized here, that the collapse of such a sheet cavity and the resulting hull pressure fluctuations and underwater radiated noise is characterized by the collapse of the closure-vortex cavity. This implies that the dynamics of vortex-cavitation are also relevant for the collapse of such a sheet cavity. This needs to be further investigated.

Examples of a closure-vortex cavity are presented in Figure 10, that shows the cavitation pattern of a single screw propeller for two blade positions as observed in the cavitation tunnel of MARIN. At blade 1 the cavity-closure vortex directly merges with the tip-vortex cavity. At blade 2, the closure-vortex cavity initially remains separate from the tip-vortex cavity and the two co-rotating vortices roll-up around each other and merge further downstream of the blade. For a large chordwise extent of the sheet cavity, the closure-vortex cavity may collapse downstream of the trailing edge. It is expected that it is the collapse of this closure-vortex cavity that determines the hull-pressure fluctuations and radiated noise.

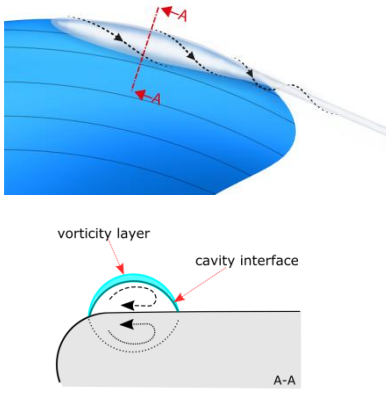

Figure 8. Schematic pattern of an attached tip-vortex cavity.

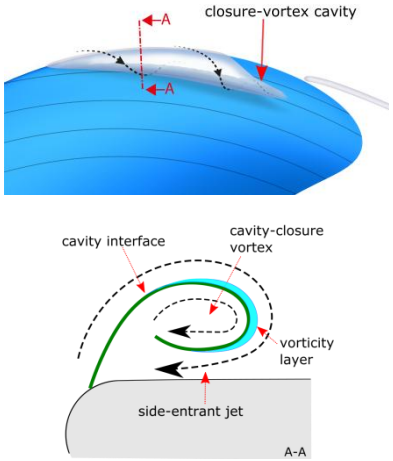

Figure 9. Schematic pattern of a closure-vortex cavity, formed by sheet cavitation.

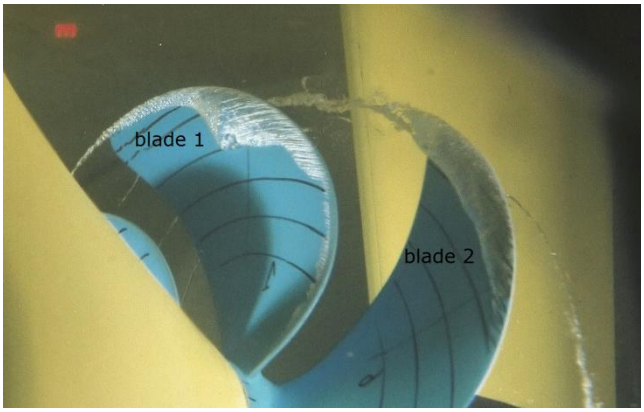

Figure 10. Example of a cavity-closure vortex that is directly connected to the tip vortex (blade 1) and a closure-vortex cavity that initially remains separate from the tip-vortex cavity (blade 2).

5 TIP-VORTEX EXCITATION MECHANISMS

5.1 Ship wake

The velocity variation in the ship wake leads to a variation in blade loading and, therefore, also to a variation in tip-vortex strength and to a variation in tip-vortex cavity size. In addition, the vortex cavity will deform under influence of the spatial and temporal velocity fluctuations due to the non-uniformity and turbulence in the ship wake. These excitation mechanisms are present for a detached tip-vortex cavity of a ship propeller.

5.2 Interaction with sheet cavity

In most situations, the tip-vortex cavity is connected to a sheet cavity on the blade which can be either a closed cavity shape (referred to above as an attached tip-vortex cavity) or an open sheet cavity with a cavity-closure vortex. As discussed above, for a small sheet cavity with the cavity-closure vortex located very close to the blade

tip, the vapour of the sheet is directly transported in the tip-vortex cavity and the tip-vortex cavity also acts as the closure-vortex cavity.

When the blade moves through the wake peak, the loading on the blade temporarily increases which first leads to an increase of the extent of the sheet cavity followed by a decrease of the extent of the sheet cavity. During the decrease of the volume of sheet cavity, the vapour part of the sheet cavity is convected into the tip-vortex cavity where it leads to an increase of the cavity diameter. As this increase in cavity diameter cannot be sustained by the tip-vortex strength, the tip-vortex cavity collapses and rebounds. Hence, if the tip-vortex cavity is connected to a sheet cavity on the blade that does not have a separate closure-vortex cavity, the collapse and rebound of the tip-vortex cavity is preceded by the transport of vapour from the sheet cavity into the tip-vortex cavity.

A series of high-speed video frames showing this mechanism is shown in Figure 11. This example shows an attached tip-vortex cavity on a propeller blade which is identical to Case 2 in Figure 7. The increase in cavity size related to the ship wake remains more or less stationary in the wake frame of reference with the blade passing through it. The maximum cavity extent showing in frame #1 is then moved in the tip-vortex cavity in frame #2 after which it collapses and rebounds.

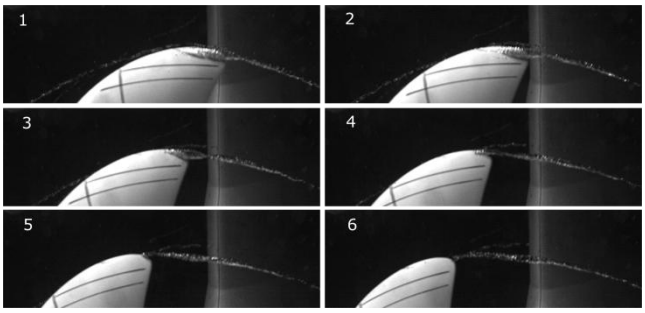

Figure 11. Series of high-speed video images showing collapse of an attached tip-vortex cavity on a podded propeller. Time between frames corresponds to an increment in blade position of 3.8 deg.

5.3 Other vortices

For a controllable pitch propeller operating at low ship speed, i.e. pitch is reduced with respect to design pitch, a vortex may emanate from the face of the blade. As the propeller is still producing thrust, a tip vortex is still generated on the back of the blade. This pair of vortices is counter-rotating and the interaction between these two vortices leads to a roll-up of the weaker vortex around the stronger vortex, ultimately leading to break-up of the weaker vortex into ring vortices. As both vortices may cavitate, the interaction between the vortices may also lead to break-up of the cavity and thereby to a collapse. This break-up mechanisms is known to lead to high broadband noise levels as discussed in the introduction.

6 CONCLUDING REMARKS

A concise review has been given of the mechanisms involved in the broadband noise of (tip-)vortex cavitation. For an attached tip-vortex cavity without significant sheet cavitation, the collapse can be excited by the transport of vapour from the sheet into the vortex cavity. When the sheet cavity grows, it is hypothesized that the sheet-cavity closure vortex forms a cavity structure that will also collapse as a vortex cavity.

Based on 2-D computations, the collapse of a vortex cavity is expected to be inertia driven and that, therefore, the effect of viscosity is small. The resulting increase in azimuthal velocity at the cavity interface dampens the collapse which ultimately results in a rebound and therefore resonance. Whether this also holds for 3-D flow needs to be further investigated. An analytical formulation for the resonance frequency could only be derived for 2-D flow.

The radiated pressure of a vortex cavity has been described by an analytical solution for a cylindrical noise source. This noise source becomes a monopole at low frequency and in the far field. In the near field, the situation is more complicated which needs to be further investigated.

It has quantitatively been shown that the variability between blade passages leads to a decrease of higher order harmonics of the blade passage frequency and to the generation of a broadband hump in the low-frequency hull-pressure spectrum. This variability needs to be further investigated from a quantitative point of view, for sea trials as well as for model tests.

REFERENCES

23rd ITTC Specialist Committee on Cavitation Induced Pressures (2002). Final report and recommendations to the 23rd ITTC. 23rd International Towing Tank Conference, Venice, Italy.

Arndt, R., Pennings, P., Bosschers, J., and van Terwisga, T. (2015). The Singing Vortex. Interface Focus, 5:2015.0025.

Baiter, H.-J., Gruneis, F., and Tilmann, P. (1982). An Extended Base for the Statistical Description of Cavitation Noise. ASME International Symposium on Cavitation Noise, Phoenix, Arizona, USA, pages 93–108.

Bark, G. (2000). Selected Problems about Scaling of Cavitation Noise at Low and Medium High Frequencies. Developments in the Design of Propulsors and Propulsion Systems. 34th WEGEMT School, Delft University of Technology, the Netherlands.

Bark, G. and Bensow, R. E. (2013). Hydrodynamic Mechanisms Controlling Cavitation Erosion. International Shipbuilding Progress, 60:345–374.

Berghult, L. (2000). Propeller Induced Tip Vortex Noise as Function of Blade Area and Blade-Tip Loading. Int. Conf. on Propeller Cavitation, NCT'50, Newcastle upon Tyne, UK.

Bosschers, J., Janssen, A., and Hoeijmakers, H.W. M. (2008). Similarity Solutions for Viscous Cavitating Vortex Cores. Journal of Hydrodynamics, Ser. B, 20(6):679–688.

Bosschers, J. (2009a). Investigation of Hull Pressure Fluctuations Generated by Cavitating Vortices. 1st International Symposium on Marine Propulsors (smp'09), Trondheim, Norway.

Bosschers, J. (2009b). Modeling and Analysis of a Cavitating Vortex in 2D Unsteady Viscous Flow. 7th International Symposium on Cavitation CAV2009, Ann Arbor, Michigan, USA.

Bosschers, J. (2018a). A Semi-Empirical Prediction Method for Broadband Hull Pressure Fluctuations and Underwater Radiated Noise by Propeller Tip Vortex Cavitation. Journal of Marine Science and Engineering 6(49).

Bosschers, J. (2018b). Propeller Tip-Vortex Cavitation and its Broadband Noise. PhD thesis, University of Twente, Enschede, The Netherlands.

Bosschers, J. (2018c). An Analytical and Semi-Empirical Model for the Viscous Flow around a Vortex Cavity. International Journal of Multiphase Flow, 105:122-133.

Brubakk, E. and Smogeli, H. (1988). QE2 from Turbine to Diesel - Consequences for Noise and Vibration. IMAS Conference, The Design and Development of Passenger Ships.

Carlton, J. S. (2015). Broadband Cavitation Excitation in Ships. Ships and Offshore Structures, 10(3):302–307.

Chahine, G. L. (1995). Bubble Interaction with Vortices. Green, S. I., editor, Fluid Vortices, pages 783–827. Kluwer Academic Publishers.

Foeth, E.-J., van Terwisga, T., and van Doorne, C. (2008). On the Collapse Structure of an Attached Cavity on a Three-Dimensional Hydrofoil. Journal of Fluids Engineering, 130(7).

Franc, J.-P. and Michel, J.-M. (2004). Fundamentals of Cavitation. Kluwer Academic Publishers

Fréchou, D., Dugué, C., Briançon-Marjollet, L., Fournier, P., Darquier, M., Descotte, L., and Merle, L. (2000). Marine Propulsor Noise Investigations in the Hydroacoustic Water Tunnel GTH. 23rd Symposium on Naval Hydrodynamics, Val-de-Reuil, France.

Friesch, J. (1998). Correlation Investigations for Higher Order Pressure Fluctuations and Noise for Ship Propellers. Third International Symposium on Cavitation, Grenoble, France.

Fujiyama, K. and Nakashima, Y. (2017). Numerical Prediction of Acoustic Noise Level induced by Cavitation on Ship Propeller at Behind-Hull Condition. Fifth International Symposium on Marine Propulsors (smp'17), Espoo, Finland.

Junger, M. C. and Feit, D. (1986). Sound, Structures, and their Interaction. The MIT Press, 2nd edition.

Kuiper, G. (2001). New Developments around Sheet and Tip Vortex Cavitation on Ships' Propeller. 4th International symposium on Cavitation, Pasadena, California, USA.

Ligneul, P., Crance, C., and Bovis, A. (1983). Tip Vortex Cavitation Noise of a Screw Propeller Theory and Experiments. Proceedings of the Second Conference on Cavitation, Edinburgh, UK.

MacFarlane, G. G. (1949). On the Energy Spectrum of an Almost Periodic Succession of Pulses. Proceedings of the Institute of Radio Engineering, 37(10):1139–1142.

Maines, B. and Arndt, R. E. A. (1997). The Case of the Singing Vortex. Journal of Fluids Engineering, 119(2):271–276.

Meleshko, V. V. and van Heijst, G. J. F. (1994). On Chaplygin's Investigations of Two-Dimensional Vortex Structures in an Inviscid Fluid. Journal of Fluid Mechanics, 272:157–182.

Okamura, N., Fujino, R., and Tanaka, T. (1994). An Experimental Investigation of the Mechanism and the Pressure of Counter-Rotating Vortices on a CPP at the Off-Design Condition. 20th Symposium on Naval Hydrodynamics, Santa Barbara, California, USA.

Pennings, P. C., Bosschers, J., Westerweel, J., and van Terwisga, T. J. C. (2015a). Dynamics of Isolated Vortex Cavitation. J. Fluid Mech., 778:288–313.

Pennings, P. C., Westerweel, J., and van Terwisga, T. J. C. (2015b). Flow Field Measurement around Vortex Cavitation. Experiments in Fluids, 56:206:1–13.

Pennings, P., Westerweel, J., and van Terwisga, T. (2016). Cavitation Tunnel Analysis of Radiated Sound from the Resonance of a Propeller Tip Vortex Cavity. International Journal of Multiphase Flow, 83:1–11.

Raestad, A. E. (1996). Tip Vortex Index - an Engineering Approach to Propeller Noise Prediction. The Naval Architect, pages 11–16.

Rosenhead, L. (1931). The Formation of Vortices from a Surface of Discontinuity. Proc. R. Soc. Lond. Ser. A, 134.

Thomson, W. L. K. (1880). Vibrations of a Columnar Vortex. Philosophical Magazine, X.

van Terwisga, T., van Wijngaarden, E., Bosschers, J., and Kuiper, G. (2007). Achievements and Challenges in Cavitation Research on Ship Propellers. International Shipbuilding Progress, 54(2-3):165–187.